Slovak Journal of Civil Engineering
Vol. 26, 2018, No. 4, 39 – 49
DOI: 10.2478/sjce-2018-0027

BEARING CAPACITY OF SLENDER CONCRETE COLUMNS

Alfred STRAUSS[1*], Thomas ZIMMERMANN[2], Panagiotis SPYRIDIS[3], Benjamin TÄUBLING[2]

Abstract

The European standard for the design of concrete structures using nonlinear methods contains a deficit in global reliability for cases when concrete columns fail due to a loss of stability before reaching the design resistance in the critical cross-sections. A buckling failure is a brittle failure which occurs without warning, and the probability of its formation is markedly influenced by the slenderness of the column. The calculation results presented herein are compared with the results from experimental data. The paper aims to compare the global reliability of slender concrete columns with a slenderness of 90 and higher. The columns are designed according to the methods stated in EN 1992-1-1, namely, a general nonlinear method and methods based on nominal stiffness and nominal curvature. The mentioned experiments also served, on the one hand, as a basis for the deterministic nonlinear modeling of the columns and, subsequently, for the probabilistic evaluation of the variability of the structural response. Finally, the results may be utilized as thresholds for the loading of the structural elements produced. The paper aims at presenting a probabilistic design that is less conservative than the classic partial safety factor-based design and alternative ECOV method.

Address

[1] University of Natural Resources and Life Sciences, Dept. of Civil Engineering and Natural Hazards, Vienna, Austria
[2] Building Inspection MA37, City of Vienna, Vienna, Austria
[3] TU Dortmund, Faculty of Architecture and Civil Engineering, Dortmund, Germany

* ***Corresponding author:*** alfred.strauss@boku.ac.at

Key words

- Bearing capacity,
- Slender concrete columns,
- Reliability of columns.

1 INTRODUCTION

The reliability method for structures is based on the use of partial safety factors when they ensure the required probability of failure. In the ultimate limit state (ULS), the effect of loads is increased by partial safety factor γ_F, and the resistance of materials is reduced by partial safety factor γ_M:

$$\gamma_F E_k \leq \frac{R_k}{\gamma_M} \tag{1}$$

EN 1992-1-1 for the design of concrete structures offers three methods for taking 2nd order effects into account (Benko, 2016; Moravcik et al., 2012; Pfeiffer, 2014), i.e., a method based on nominal curvature, a method based on nominal stiffness, and a general nonlinear method. The buckling failure of compressed slender concrete members can, however, overtake the reaching of the material's resistance in the critical cross-section (Benko, 2016). In these cases the definition of a partial safety factor for a buckling failure is appropriate, because the partial safety factors of the materials influence the reliability of the overall design to a lesser extent. Thus far, only the Austrian national documents recommend the partial safety factor for stability failure (Benko et al., 2016).

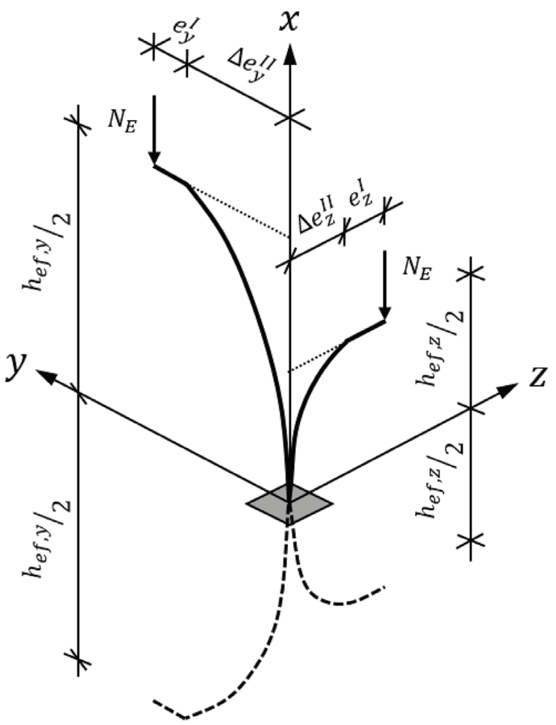

Fig. 1 *Static substitute system of the compression member (Förster, 2018)*

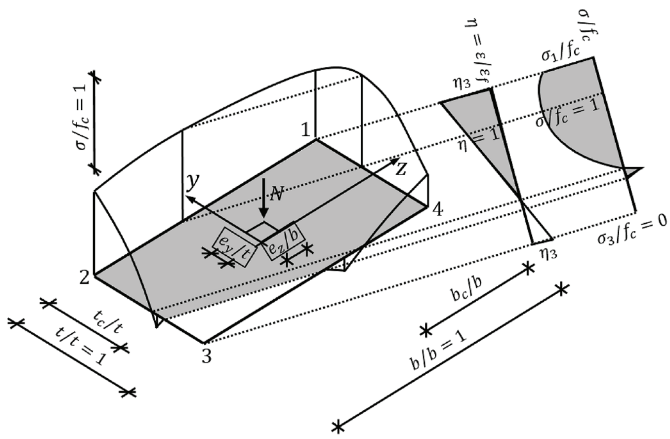

Fig. 2 *Stress and strain distribution of a cross-section (Benko, 2001); t,b are the cross sectional dimensions of the column in directions y and z respectively, and the curved prism represents the asymmetrical stress distribution σ in the x axis, due to the eccentricities $e_{y\ and}\, e_z$*

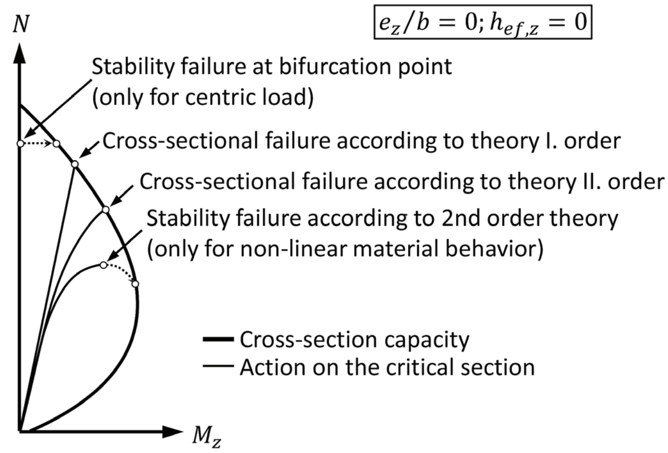

Fig. 3 *Interaction of moments and normal forces of centrically and uniaxially eccentrically loaded compression members (Benko, 2001)*

2 GENERAL DESIGN METHODS

2.1 Capacity of compressive loaded slender columns

A combination of acting compressive normal forces with bending moments around two axes can be mapped by a two-axis eccentric normal force. The associated universal static substitute system with different buckling lengths in both directions ($h_{ef,y}$ and $h_{ef,z}$) is shown in Fig. 1. Besides the eccentricities of the normal force (e^{I}_{y} and e^{I}_{z}), the deformations resulting from the 2nd order theory (Δe^{II}_{y} and Δe^{II}_{z}) also have to be taken into account.

Since concrete only has a very low tensile strength, cracks in the cross section depend on the eccentricities of the load. In this case, the overpressed cross-sectional area may be pentagonal, quadrilateral, or triangular, as seen in Fig. 2, which shows the relative stress and strain distributions of a cracked cross section with a pentagonal pressure zone (i.e., when the stress prism intersects with only one edge of the cross section)

For calculating the load-bearing capacity for compression members, it is always necessary to take into account the effects of deformations in the event that the compact elements are not infinite. The moment-normal force interactions of uniaxially eccentrically loaded compression members are shown in Fig. 3. The outer curve corresponds to the bearing capacity of the cross-section. If the actions are considered according to the 1st order theory in the critical section (fixed support, see Fig. 1), the cross-sectional bearing capacity is always achieved, and there is a linear relationship between the normal force and the bending moment. If the resulting deformations are taken into account, the bending moment increases disproportionately as the normal force increases (cross-sectional failure to the 2nd order theory). In the case of compact concrete compression elements, the cross-sectional bearing capacity is still achieved despite possible cracking in the deflected state. In the case of slender compression, the load is increased due to the significant reduction in the disproportionate crack-related stiffness. The equilibrium state (stability of the system) is reached within the interaction curve for cross-sectional failure.

2.2 Procedure for determining bearing capacity

2.2.1 Theoretical calculation methods

(a) *Centrically loaded compressive elements:* The most important basis for calculating compression elements was done by Euler. He assumed a sinusoidal deformation over a column's length. The mean critical normal force (the Euler load) is calculated through the following equations:

$$N^{II}_{crit,m} = \frac{\pi^2 \cdot EI_z}{h_{ef,y}{}^2}\ bzw.\ \Phi^{II}_{crit,m} = \frac{\pi^2}{12 \cdot \lambda_y{}^2} \tag{2}$$

$$with\ \lambda_y = \frac{h_{ef,y}}{t} \cdot \sqrt{\varepsilon_f} \tag{3}$$

The load factor Φ^{II}_{crit} describes the average system's load capacity based on the average compressive strength f_{cm} and the cross-sectional area. It depends on a material-specific slenderness ($\lambda_y = h_{ef,y} / t \cdot \varepsilon_f^{1/2}$) that uses the strain ε_f at a maximum stress. The branching load of a centrically loaded column made of tensile material is always within the curve of the cross-sectional bearing capacity (see Fig. 3); hence this special case can also be regarded as a stability failure (see Fig. 4). Since Euler presupposed unrestricted linear-elastic material behavior, the branching load tends to the infinite for the compact compressive elements. Navier recognized that in addition to stability failure, cross-sectional failure according to the 2nd order theory may also occur. However, this was only generally known through the experiments of Tetmajer (Kollbrunner and Meister, 1961). To limit the stresses, Navier proposed a straight-line equation, which could be interpreted as a load factor:

$$\Phi_{Rm}^{II} = 1.0 - 0.0139 \cdot \frac{h_{ef,y}}{t} \tag{4}$$

Engesser (1889) was able to calculate the load-bearing capacity of compact elements with tensile material using a buckling module instead of Euler's stiffness. In this case, the buckling module is composed of moments of inertia of the compression and tension zones as well as a modulus of elasticity depending on the material behavior and on strain at the ULS. This approach can be used to model the load-bearing capacity of compact and slender compression elements. Fig. 4 illustrates the related systemic load capacity of a compression member made of tensile material in the form of the load factor as a function of the material-normalized slenderness. The Euler-hyperbola, the Navier or Tetmajer line as well as the load capacities according to Engesser are plotted. For compacted compression elements whose slenderness is smaller than the limit slenderness $\lambda_{y,lim}$, cross-sectional failure occurs according to the 2nd order theory, and with increasing slenderness, the branch load (stability failure) becomes relevant.

Haller (1949) studied the load-bearing capacity of uniaxially and eccentrically loaded unreinforced masonry walls with any stress-strain relationship. He reduced the determination of the load capacity at the critical section to the equilibrium condition by assuming a sinusoidal profile of the curvatures over a bar's height. The total eccentricity in the critical section can be determined on the basis of the curvature, which can be determined with the strain-difference (ε_1-ε_4) and the wall thickness t (Haller 1949):

$$e_y^{II} = e_y^I + \Delta e_y^{II} = e_y^I + \frac{{h_{ef,y}}^2}{\pi^2} \cdot \kappa_z, with\ \kappa_z = \frac{\varepsilon_1 - \varepsilon_4}{t} \tag{5}$$

The load factor can be calculated for rectangular cross-sections with the coefficient of the imperfection α_R of the stress-strain relationship and the related overpressed length t_c / t, as follows (Haller 1949):

$$\Phi_{Rm}^{II} = \alpha_R \cdot \frac{t_c}{t} \tag{6}$$

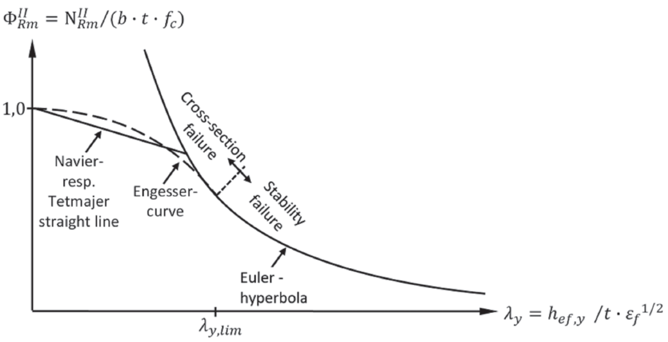

Fig. 4 *Load-bearing capacity of centrically loaded compression members (Benko, 2001)*

In addition to the shape of the stress-strain relationship, both the coefficient of imperfection α_R and the overpressed depth t_c also depend on the strain distribution over the cross-section; therefore, the system's load capacity can generally only be determined by iteration.

Kirtschig et al. (1975) used a parabolic stress-strain relationship in the Haller model and ignored tensile strength. Under this boundary condition, the bearing capacity for cross-sectional failure according to the 2nd order theory can be given as a mathematically closed relationship for the cracked sections. Kirtschig calculated the system load, which is relevant for stability failures, only iteratively. Based on these findings, he developed an approximate solution for the load factor ($\Phi^{II}_{Rd} = N^{II}_{Rd} / (b \cdot t \cdot f_{cd})$ based on the design value of the compressive strength, which is still used today in construction, see EN 1996-1-1.

$$\Phi_{Rd}^{II} = \left(1 - 2 \cdot \frac{e_y^I}{t}\right) \cdot e^{-\frac{u^2}{2}} \text{ with } u = \frac{\frac{h_{ef,y}}{t} \cdot \sqrt{\frac{f_k}{E}} - 0.063}{0.73 - 1.17 \cdot \frac{e_y^I}{t}} \tag{7}$$

For the first time, Glock (2004) presented closed solutions for the systemic load capacity of slender and compact compression elements with linear-elastic material behavior with and without consideration of the tensile strength. Further, he showed that in the case of stability failure, Euler's solution could be transferred to eccentrically stressed columns:

$$\Phi_{Rm,Stabi}^{II} = \frac{\pi^2 \cdot \left(1 - 2 \cdot \frac{e_y^I}{t}\right)^3}{12 \cdot {\lambda_y}^2} \tag{8}$$

For non linear material behavior, Glock (2004) developed a numerical calculation model. This serves as the basis for a computational approach that can be used to determine the bearing capacity of unreinforced compression members by taking into account various compliances of the stress-strain relationship, including the detection of flexural tensile strength. The method, which realistically models both cross-sectional and stability failures, is suitable for determining the bearing capacity of concrete and masonry components with uniaxial bending stress.

In his work on the load-bearing capacity of uniaxial, eccentrically loaded pressure elements Bakeer (2016) uses Glock's approach on stability failure. For cross-sectional failure he extended the parabolic approach by Johnson et al. (1916). This method can be found in the latest proposal for the revision of EN 1996-1-1.

$$\Phi_{Rm,y}^{II} = \begin{cases} \Phi_{y,pl}^I - \dfrac{\left(\frac{h_{ef,y}}{t} \cdot \sqrt{\frac{f_k}{E}}\right)^2}{3.15 \cdot \Phi_{y,pl}^I} & for\ \lambda_{y.lim} < \Phi_{y,pl}^I \cdot 1.26 \\ \dfrac{0.79 \cdot \left(\frac{h_{ef,y}}{t} \cdot \sqrt{\frac{f_k}{E}}\right)^3}{{\lambda_y}^2} & for\ \lambda_{y.lim} < \Phi_{y,pl}^I \cdot 1.26 \end{cases} \tag{9}$$

$$mit\ \Phi_{y,pl}^I = 1 - 2 \cdot \frac{e_y^I}{t}$$

(b) *Biaxial bending elements:* For determining the load capacity of non-reinforced pressure elements made of mineral material under a biaxial eccentric load, only rudimentary information can be found in the literature. A scientifically proven theoretical solution is still pending. The load-bearing capacity of reinforced concrete pressure elements under oblique bending can be solved without numerical finite element (FE) calculations only for a few simple cases or by using special interaction diagrams (Allgöwer, 2001 and Quast, 2004).

2.2.2 Normative regulations for concrete pressure members

(a) *Uniaxially bending-stressed compression members:* The design of exclusively uniaxial, eccentrically stressed compression members may be simplified in accordance with EN 1992-1-1 (2004) with Eq. (10). The load factor ($\Phi^{II}_{Rd,y} = N^{II}_{Rd,y} / (b \cdot t \cdot f_{cd})$) depends linearly on the slenderness $h_{ef,y}/t$. The maximum value ($1 - 2 \cdot e^{I}_{y}/t$) defined in equation (10) corresponds to the cross-sectional capacity for rigid-plastic material behavior without any consideration of the tensile strength.

$$\Phi^{II}_{Rd,y} = 1.14 \cdot \left(1 - 2 \cdot \frac{e^{I}_{y}}{t}\right) - 0{,}02 \cdot \frac{h_{ef,y}}{t} \leq 1 - 2 \cdot \frac{e^{I}_{y}}{t} \qquad (10)$$

(b) *Biaxial bending-stressed compression members:* Under certain circumstances, in the case of biaxial eccentrically-loaded compression members according to EN 1992-1-1, both main directions may be calculated separately without taking into account the effects of oblique bending. The system's load capacity corresponds to the smaller of the two load capacities determined. This rule was developed for reinforced concrete elements. However it is also valid for unreinforced compression elements, and the limits according to Eqs. (11) and (12) (see white triangles in Fig. 5), must be taken into account.

$$0.5 \leq \delta = \frac{h_{ef,y}/t}{h_{ef,z}/b} = \frac{h_{ef,y} \cdot b}{h_{ef,z} \cdot t} \leq 2.0 \qquad (11)$$

$$0.2 \leq \psi^{I} = \left|\frac{e^{I}_{z}/b}{e^{I}_{y}/t}\right| \leq 5.0 \qquad (12)$$

If the referenced eccentricity in the direction of the width is $e^{I}_{z}/b > 0.2$, the calculated reduced cross-sectional width $b_{red,EC2}$ must be taken into account according to the German NA of DIN EN 1992-1-1 (2004):

$$\frac{b_{red,EC2}}{b} = \frac{1}{2} + \frac{1}{12 \cdot \frac{e^{I}_{z}}{b}} \leq 1.0 \qquad (13)$$

Even though it has a different quantity, the computational reduction of the cross-sectional width corresponds to the procedure of the German NA of DIN EN 1996-1-1 by multiplying the load factors $\Phi^{II}_{Rd,Sys} = \Phi^{II}_{Rd,y} \cdot \Phi^{I}_{Rd,z} = \Phi^{II}_{Rd,y} \cdot (1 - 2 \cdot e^{I}_{z}/b)$.

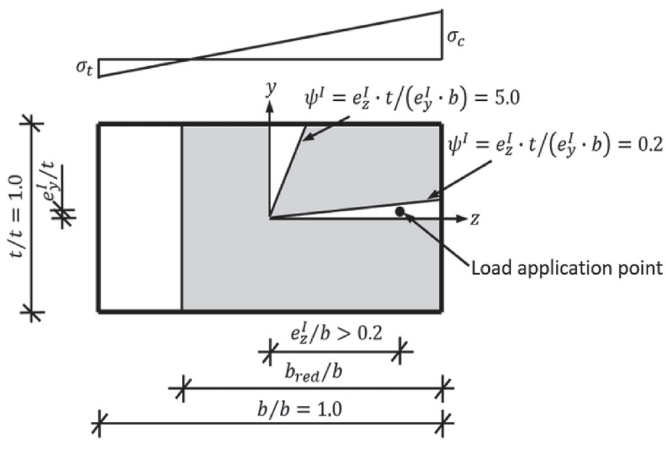

Fig. 5 *Calculated reduction in the width of the cross-section for positive eccentricities according to DIN EN 1996-1-1*

2.3 Analysis of a system's load capacity according to different approaches

The design values of a system's capacities can be determined based on the following calculation methods:

1. Realistic non linear calculations, taking into account the eccentricities in both directions
2. Calculations without any correction factor using the uniaxial load capacities from a non linear calculation
3. Calculations without any correction factor using the uniaxial load capacities according to EN 1992-1-1 (eq. (9))
4. Calculations according to the German NA of EN 1992-1-1 based on separate proofs in the axial directions (eqs. (10) with (13))
5. Calculations according to the German NA of EN 1992-1-1 based on the moment interaction

In addition to the approaches outlined here, there are also opportunities in the new Eurocode generations for non linear numerical in-depth procedures. These methods as well as the experimental studies in the interaction diagrams (see Fig. 3) show some effects that do not completely fulfill the safety requirements. These are highlighted in the following sections.

3 ADVANCED VERIFICATION OF SLENDER CONCRETE COLUMNS

3.1 Experimental setup

The task of the experiments was to design the geometry and reinforcement of the columns together with the initial eccentricity of the axial force in such a way that the columns would collapse due to the loss of stability inside the interaction diagram, i.e., before achieving the design resistance in the critical cross-section with an approximate compressive strain in concrete ε_{c1} = 1.5 ‰ (Benko et al., 2016). The force and the initial eccentricity e_1 for the buckling failure were determined using non linear calculations with the Stab2D-NL software. The standard characteristics of the C45/55 material and B500B steel were used in these calculations. The experimentally verified concrete columns had a rectangular cross-section with dimensions of 240 x 150 mm. The total length of the columns with spread steel plates was 3840 mm. The columns were reinforced with four Ø14 mm diameter bars. These four bars were supplemented with another four bars with a diameter of Ø14 mm and a length of 600 mm on both ends of the columns. The supplementary bars were welded to steel plates with a thickness of 20 mm. The transverse reinforcement consisted of two leg stirrups with a diameter of Ø 6 mm. As the local failure in the ending parts can precede the stability collapse of the columns, the resistance was increased by doubling the transverse reinforcement along the length of the additional bars; (Benko et al., 2016) provides further details.

3.2 Experimental results

After the production of the experimental samples and preparation of the laboratory conditions, the concrete columns were tested in the laboratory of the Civil Engineering Faculty of SUT Bratislava. During the experiments, measurements were taken on both sides of the concrete cross-section. The results of the experiments are in Benko et al. (2016). Despite the fact that the columns were fabricated using the same materials and with great attention paid to accuracy, the differences in the results are notable. The major difference in the buckling force reaches 15.9%, whereas in deformations of the columns in the middle (e^2), it goes up to 44.9%. The measurements were taken on 6 testing samples of slender concrete columns (Benko et al., 2016).

3.3 Reliability of columns – loss of stability

Fig. 6 shows a comparison of the results for the experimentally verified S1-1 to S1-6 columns. The group of results from the non linear calculations calibrated to the mean values of the material characteristics acquired from the experiments is marked with a thick line. The axial force at the stability loss is then 306.5 kN. When assuming the characteristic values of the material characteristics, the axial force at the loss of stability is 279.9 kN (characteristic). Finally, when assuming the design values of the material characteristics, the axial force is 240.0 kN (design). According to the method based on nominal stiffness, the maximal resistance of the column with a slenderness of λ=89 is 205.0 kN (stiffness). The maximal resistance is the point where the stiffness curve intersects the design interaction diagram. According to the method based on the nominal curvature (EN 1992-1-1), the resistance of the column is 153.0 kN (curvature). Tab. 1 summarizes the partial reliability factors for the loads and materials and also the overall reliability factor. The overall reliability of the design according to the method based on nominal curvature is 1.57 times higher than the reliability of the non linear method according to EN 1992-1-1.

3.4 Reliability of columns – parametric study slenderness λ = 89 to 160

The differences in the reliability of the design methods according to EN 1992-1-1 for a slenderness of λ = 160 and the initial eccentricity of e_1 = 40 mm are shown in Fig. 7. The resulting values for the column's resistance and the partial reliability factors for the loads and materials together with the overall reliability factors of the above-stated design methods are in Tab. 2.

3.5 Probabilistic analyses

The SARA GUI environment along with the ATENA solver and FReET reliability tool (Novak et al., 2014) were used for the stochastic analysis in order to estimate the statistical variability of the Normal-Moment capacity of the slender columns discussed and to propose probabilistic-based design values or resistances. A sensitivity analysis performed at the beginning of the whole process showed the most decisive/dominating parameters of the non linear modeling. A set of 12 parameters was utilized for a stochastic evaluation of the variability of the structural response. The stochastic model of the concrete was based on data presented in (Routil et al., 2014; Strauss et al., 2014; Zimmermann et al., 2014; Zimmermann et al., 2016), and was obtained by ANN-based identification (Lehky et al., 2014; Zimmermann and Lekhy, 2014).

Tab. 1 *Comparison of the reliability of columns; λ=89 and e_1=40mm; the overall safety factor is calculated as the product of the partial safety factors as a principle of the LRFD design*

overall reliability to the characteristic values of the material properties	Axial force [kN] design	Axial force [kN] characteristic	γ_F load	γ_M material	γ_o overall
characteristic	279.9	-	1.40	1.00	-
design	240.0	171.4	1.40	1.17	1.63
stiffness	205.0	146.4	1.40	1.37	1.91
curvature	153.0	109.3	1.40	1.83	2.56

Tab. 2 *Comparison of the reliability of columns; λ=160 and e_1=40mm; the overall safety factor is calculated as the product of the partial safety factors as a principle of the LRFD design*

overall reliability to the characteristic values of the material properties	Axial force [kN] design	Axial force [kN] characteristic	γ_F load	γ_M material	γ_o overall
characteristic	99.0	-	1.40	1.00	-
design	90.0	64.3	1.40	1.10	1.54
stiffness	68.0	48.6	1.40	1.46	2.04
curvature	48.0	34.3	1.40	2.06	2.89

The material parameters of the concrete identified were obtained from a laboratory test under perfect conditions, which resulted in quite small variations of the material parameters of the concrete. In order to ensure realistic results, it was necessary to introduce a higher degree of variability for the material parameters obtained and to also

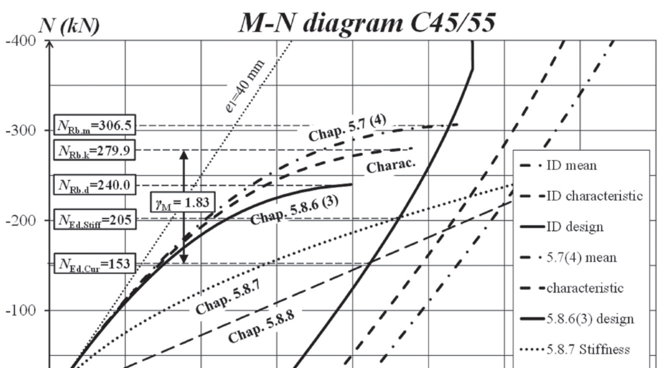

Fig. 6. *Reliability of the columns according to loss of stability; λ = 89 and e_1 = 40mm (Benko et al., 2017)*

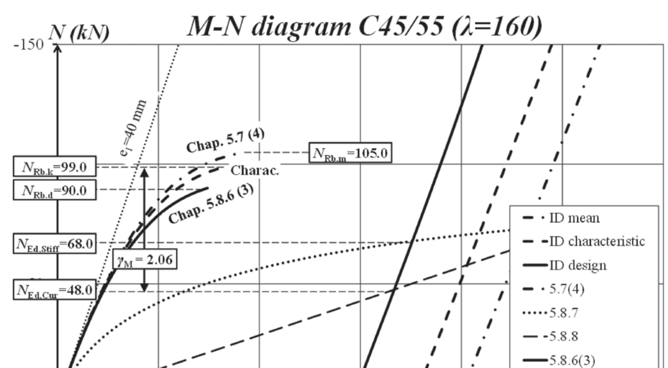

Fig. 7 *Reliability of the columns according to loss of stability – λ = 160 and e_1 = 40mm (Benko et al., 2017)*

Tab. 3 *Stochastic model of the destructive test*

Parameter	Mean	COV [%]	PDF	Unit
Steel reinforcement (Bars and stirrups)				
E	200	2	Normal	[GPa]
f_{ys}	500	5	Normal	[MPa]
Concrete C45/55				
E	38.17	18	Weibull min (3 par)	[GPa]
f_t	3.471	15	Gumbel Max. EV I	[MPa]
f_c	-46.75	6	Gumbel Min. EV I	[MPa]
G_f	8.677E-05	22	Gumbel Max. EV I	[MN/m]
r	0.0023	4	Normal	[kton/m³]

randomize the density of the concrete mixture. The non linear modeling of the experiment performed showed some variability in the reinforcing effects around the value calculated. Due to the small number of experimental samples, it was not possible to make a reliable assessment; therefore, the recommendations of the JCSS regarding the uncertainties were adopted. The whole stochastic model of the destructive tests of the columns is shown in Tab. 3, whereby *E* and the correlation matrices utilized are presented in Tabs. 4 to 7.

3.6 Probabilistic assessment

Due to the enormous computational demands of such a study, it was necessary to utilize the efficient HSLHS (Vorechovsky, 2014) of concrete. This approach permits extending the number of simulations performed after previously performed runs of the LHS simulations. The aim is to perform an analysis with a lower number of samples generated at the beginning to fix possible errors and to use previous simulations in cases where no errors occur.

The statistics of the response of the above-described columns using a set of 11 simulations extended to a second run of the HSLHS method by an additional 20 simulations. The response of the assessed structural members was evaluated for two limit states, i.e., **(I) the Ultimate limit state** represented by the critical value of the force applied during the experiment (peak of the LD diagram) and **(II) the Service limit state** represented by the value of the force at the moment when the first bending cracks occur. A lognormal probability distribution is assumed for both limit states. In the case of a fully probabilistic design, the percentile of the N-M resistance calculated corresponds to a probability of 0.0012 according to the recommendations in EN 1990 (based on the separation of the resistance and the action of the load variables). Fig. 8 shows a comparison of the 31 LD curves for the simulations calculated.

The estimated probability function (PDF) of the N/M resistance is shown in Fig. 9. The structural response was considered to be log-normally and normally distributed respectively.

4 PROBABILISTIC DESIGN AND SAFETY FORMATS

4.1 Semi-probabilistic approach

In practical applications nonlinear finite element models amount to huge calculation efforts, and stochastic models contain a high number of randomly input variables. In such cases, the computational requirements are significantly reduced by semi-probabilistic methods, where the design value of response *R* is evaluated instead of the probability of failure. If *R* is a lognormal distributed independent random variable, the design value of *R* is defined as:

$$R_d = \mu_R \cdot exp(-\alpha_R \beta_n v_R) \tag{14}$$

where is the coefficient of the variation (CoV); α_R represents the sensitivity factor; and the recommended value is $\alpha_R = 0.8$. The reliability index β is another way to express the probability of failure p_f and is defined by:

$$\beta = -\Phi_N^{-1}\left(p_f\right) \tag{15}$$

Tab. 4 *Correlation of parameters for concrete, Series 1*

	E	f_t	f_c	G_f	ρ
E	1	0.60	-0.70	0.80	0
f_t		1	-0.90	0.50	0
f_c			1	0.70	0
G_f				1	0
r					1

Tab. 5 *Correlation of parameters for concrete, Series 2*

	E	f_t	f_c	G_f	ρ
E	1	0.48	-0.56	0.64	0
f_t		1	-0.72	0.40	0
f_c			1	0.56	0
G_f				1	0
r					1

Tab. 6 *Correlation of parameters for concrete, Series 3*

	E	f_t	f_c	G_f	ρ
E	1	0.36	-0.42	0.48	0
f_t		1	-0.54	0.30	0
f_c			1	0.42	0
G_f				1	0
ρ					1

Tab. 7 *Correlation of parameters for concrete, Series 4 (no correlation)*

	E	f_t	f_c	G_f	ρ
E	1	0	0	0	0
f_t		1	0	0	0
f_c			1	0	0
G_f				1	0
r					1

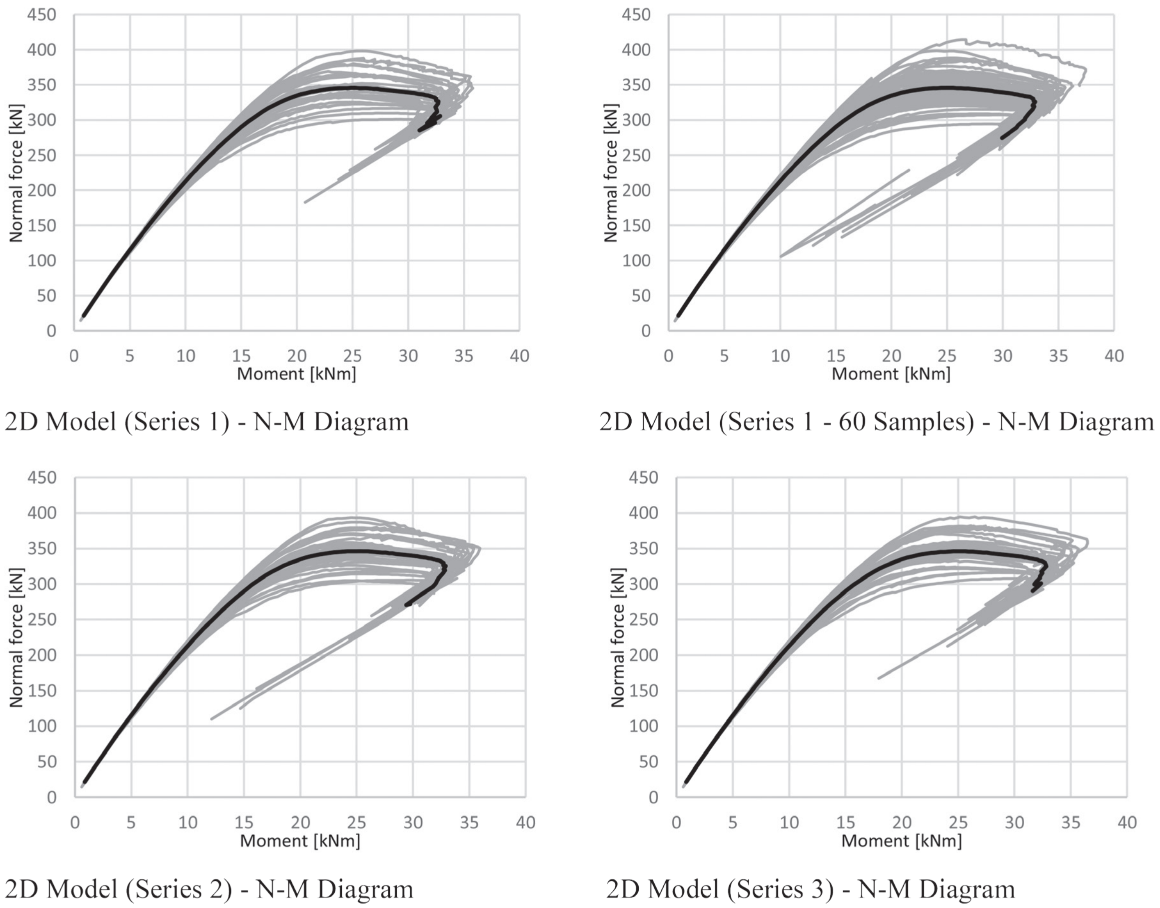

Fig. 8 *N-M Diagrams of the stochastic models*

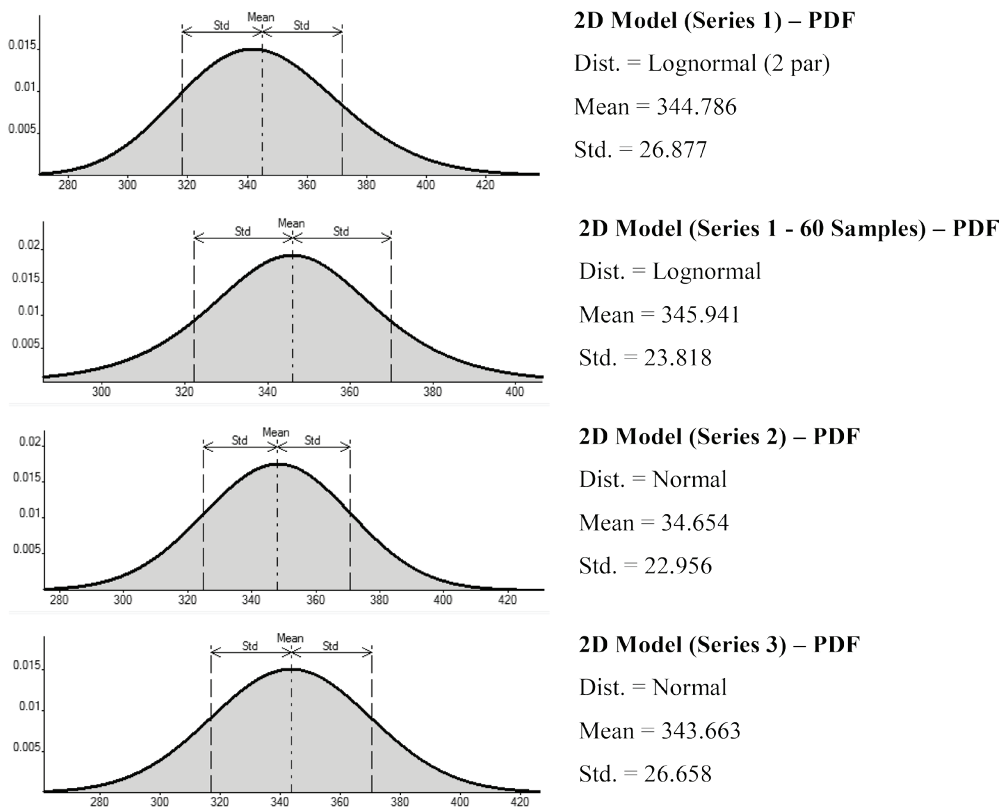

Fig. 9 *PDF of the force applied at the ultimate limit state (in kN – horizontal axis). The PDFs are fitted to the results presented in Fig. 8*

where Φ_N^{-1} is the inverse of the standard normal probability distribution function. The target reliability index for the ultimate limit state, the moderate consequences of failure, and the reference period of 50 years are set as $\beta_n = 3.8$ according to the Joint Committee on Structural Safety (JCSS).

Obviously, for a determination of the design value by a semi-probabilistic approach, it is crucial to correctly estimate the mean value and CoV; this can be done by various reliability methods. Besides a full probabilistic method using Monte Carlo-type sampling, it is possible to use more efficient sampling methods, e.g., the Latin Hyper Cube Sampling (LHS) method.

4.2 Partial safety factor

According to EN 1990, Non Linear Finite Element Analysis (NLFEA) is computed with the design values of the input random variables, and the result is assumed to be a design value of resistance R_d:

$$R_d = R(f_{yd}, f_{cd}, \dots) \tag{16}$$

The partial safety factor (PSF) method may lead to an unrealistic redistribution of internal forces and different failure modes of the structure because of the extremely low design values of the input variables. Due to the possibility of the different behaviour of the FE-model, it is recommended to compute NLFEA with the mean value and apply the global safety factor to the result.

4.3 EN 1992-2

The only global safety factor approach defined in the Eurocodes is a concept according to EN 1992-2; the design value is estimated as follows:

$$R_d = \frac{R(f_{ym}, \tilde{f}_{cm}, \dots)}{\gamma_R} \tag{17}$$

where $\tilde{f}_{cm} = 0.843 \cdot f_{ck}$ is the mean value of the steel reinforcement; $\tilde{f}_{cm} = 0.843 \cdot f_{ck}$ is the reduced mean value of the concrete's property because of its higher variability and the idea that the design values should correspond to the same probability. These values are derived from the characteristic values (5% percentile) X_k. The global safety factor for resistance is set at $\gamma_R = 1.27$. EN 1992-1-1 only allows a compressive type of failure for concrete; however, the study presented by Cervenka (2014) also extended the application to brittle modes of failure. As can be seen, the PSF and EN 1992-2 methods need just one NLFEA simulation.

4.4 ECoV by Červenka

The ECoV methods are based on a semi-probabilistic approach; the difference is in how to estimate the coefficient of the variation and the mean value of the response. A lognormal distribution for the response variable R is assumed in the proposal by Cervenka (2013) and Holicky (2006); thus the coefficient of variation v_R can be estimated as:

$$v_R = \frac{1}{1.65} \ln\left(\frac{R_m}{R_k}\right) \tag{18}$$

Note that in ECoV by Cervenka (2013) just 2 simulations of NLFEA are needed, i.e., the first one with mean values of the input random variables $R_m = R(f_{ym}, f_{cm}, a_{non} \dots)$ and the second simulation R_k using characteristic values. The concept described was adopted in the fib (2013), and the design value R_d was later decreased by another factor $\gamma_{Rd} = 1.06$:

$$R_d = \frac{R_m}{\gamma_R \gamma_{Rd}}, \quad \gamma_R = \exp(\alpha_R \beta v_f) \tag{19}$$

4.5 ECoV by Schlune et al.

The extended ECoV method was proposed by Schlune et al. (2011); v_R is composed of the variability of the numerical model v_m, geometrical uncertainties v_g, and material uncertainties v_f:

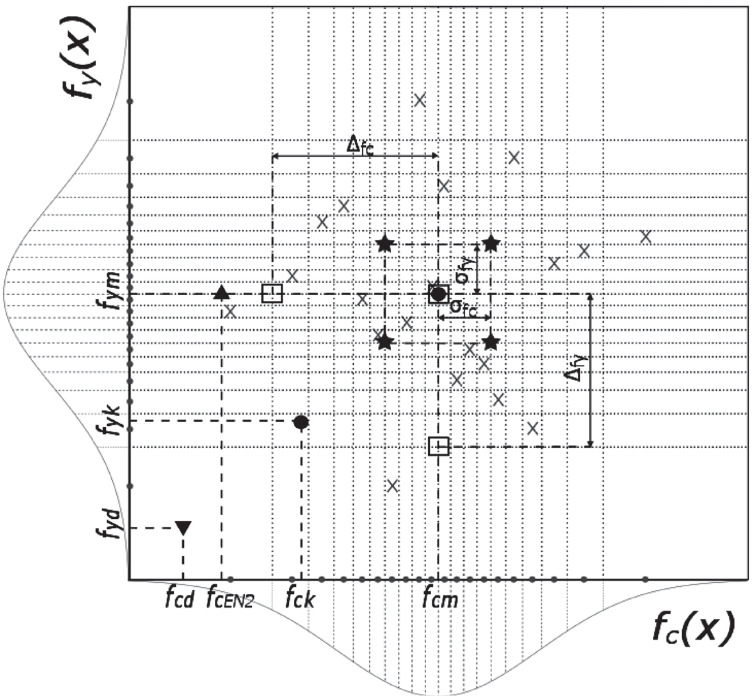

n	SAMPLING POINTS
x	X Latin Hypercube Sampling
1	▼ Partial Safety Factor
1	▲ EN 1992 - 2
2	● ECoV by Červenka
3	□ ECoV by Schlune et al.
4	★ Numerical Quadrature

Fig. 10 *Sampling points in 2D*

$$v_R = \sqrt{v_g^2 + v_f^2 + v_m^2} \tag{20}$$

The recommended values for the variability of NLFEM and the geometric uncertainties can be found in the literature. The coefficient of variation of the material v_f if the material parameters are not correlated can be calculated as:

$$v_f \approx \frac{1}{R_m} \sqrt{\sum_{i=1}^{N} \left(\frac{R_m - R_{\Delta fi}}{\Delta_{fi}} \sigma_{fi} \right)^2} \tag{21}$$

where the response of construction $R_{\Delta fi}$ is determined by NLFEA using the reduced mean values of the material variables by Δ_{fi}, and σ_{fi} is the standard deviation of the *i-th* variable. If the lognormal distribution of the material variables is assumed, the reduced values of Δ_{fi} can be calculated as:

$$f_{\Delta i} = f_{mi} \cdot exp(-c \cdot v_{fi}) \tag{22}$$

where f_{mi} is the mean value of the material characteristic and the step size parameter is defined as $c = (\alpha_R \beta)/\sqrt{2}$. Note that this approach requires N+1 simulations of NLFEA, where N is the number of material random variables. The extension of the method for the correlated material variables can be found in Schlune et al. (2011).

4.6 Sampling points in 2D

A representation of the methods described can be seen in Fig. 10. The single approaches define the sampling points in the N-dimensional space, where their coordinates represent the values of the random material characteristics input. The difference lies in the number and position of the sampling points. Generally, more sampling points lead to a more accurate estimation of the CoV, and the choice of the most efficient method depends on the size of the NLFEM and stochastic model implemented. Note that the computational requirements of the ECoV method by Schlune et al. (2011) and the numerical quadrature by Rosenblueth (1981) are strongly dependent on the size of the stochastic model. Thus a sensitivity analysis should be performed to reduce the number of random variables input.

5 SUMMARY

The global reliability of slender columns according to a non linear design method is several times lower than the global reliability of slender columns according to a method based on a nominal stiffness or nominal curvature.

The user of non linear software can result in yet another reduction of the global reliability when entering the input data for non linear calculations. This mainly applies in cases when the aim of the design is the minimization of the dimensions and the saving of material. This is often the main criterion for the free market in the European Union. The difference in the axial force of the predictions of the results within the planned experiments was 23%, and the difference between the maximal force within the non linear calculations and experimentally verified columns was 41% (Benko, 2016).

In cases when the buckling failure governs the design, the non linear method according to EN 1992-1-1 for slender columns poses limitations in its incorporation with material reliability concepts. Based on the cases demonstrated herein, it is evident that the standard requires revisions for this domain with an expansion to buckling-specific verifications for the reliability index and probability of failure.

REFERENCES

Allgöwer, G. (2001) *Bemessung von Stahlbetondruckgliedern unter zweiachsiger Biegung mit Interaktionsdiagrammen nach Theorie II. Ordnung (Design of reinforced concrete under biaxial bending with interaction diagrams according to second-order theory)*. Cottbuss: Dissertation, Brandenburgische Technische Universität.

Bakeer, T. (2016) *Empirical estimation of the load bearing capacity of masonry walls under buckling – Critical remarks and a new proposal for the Eurocode 6*. Construction and Building Materials 113, pp. 376–394.

Benko, V. (2001) *Nichtlineare Berechnung von Stahlbetondruckglieder. (Nonlinear analysis of reinforced concrete compression members).* In: Innovationen im Betonbau 27. Fortbildungsveranstaltung, OVBB Heft 47, pp. 9–12.

Benko, V., Kendický, P., Gúcky, T. (2016) *Failure of Slender Concrete Columns of Loss of Stability.* Key Engineering Materials, 691, 185.

Benko V., Valasik A., Cuhak M., Taubling B., Strauss A. (2017) *Reliability Based Performance Prediction of Slender Concrete Columns at the Loss of Stability*. In: Bucher, C., Ellingwood, B.R. and Frangopol, D.M. (eds.) Safety, Reliability, Risk, Resilience and Sustainability of Structures and Infrastructure Proceedings of the 12th International Conference on Structural Safety and Reliability (ICOSSAR2017), Vienna, Austria, 6–10 Aug. 2017.

Červenka, J., Červenka, V., Pukl, R. (2014) *Application of global safety formats from model code 2010 for design and structural assessment by non-linear analysis.* In: 4th International fib Congress 2014: Improving Performance of Concrete Structures, FIB 2014 - Proceedings, pp. 245-247.

Červenka, V. (2013) Reliability-based non-linear analysis according to fib Model Code 2010. Structural Concrete, 14(1), 19-28.

DIN EN 1992-1-1/NA (2013) *Bemessung und Konstruktion von Stahlbeton- und Spannbetontragwerken. Teil 1-1: Allgemeine Bemessungsregeln und Regeln für den Hochbau. (Eurocode 2: Design of concrete structures - Part 1-1: General rules and rules for buildings)*

DIN EN 1996-1-1 (2010) *Bemessung und Konstruktion von Mauerwerksbauten - Teil 1-1: Allgemeine Regeln für bewehrtes und unbewehrtes Mauerwerk. (Eurocode 6: Design of masonry structures - Part 1-1: General rules for reinforced and unreinforced masonry structures)*

DIN EN 1996-1-1/NA (2012) *Bemessung und Konstruktion von Mauerwerksbauten - Teil 1-1: Allgemeine Regeln für bewehrtes und unbewehrtes Mauerwerk. (Eurocode 6: Design of masonry structures - Part 1-1: General rules for reinforced and unreinforced masonry structures)*

CEN EN 1992-1-1 (2004) *Design of concrete structures - Part 1-1: General rules and rules for buildings.*

CEN EN 1990 (2002) *Basis of structural design*.

CEN EN 1992-2 (2012) *Concrete Bridges – Design and detailing rules.*

Engesser, F. (1889) *Die Knickfestigkeit gerader Stabe*. *(Buckling resistance of straight bars)* Zeitschrift des Architekten- und Ingenieur-Vereins zu Hannover.

fib federation internationale du beton / International Federation for Structural Concrete (2013) fib Model Code for Concrete Structures 2010. ISBN: 9783433030615

Förster, V. (2018) *Tragfahigkeit unbewehrter Druckglieder aus Beton und Mauerwerk bei zweiachsig exzentrischer Beanspruchung (Load-bearing capacity of unreinforced concrete compression members under biaxially eccentric loading)*. Dissertation, Institut für Massivbau, Technische Universität Darmstadt.

Glock, C. (2004) *Traglast unbewehrter Beton- und Mauerwerkswände. Nichtlineares Berechnungsmodell und konsistentes Bemessungskonzept für schlanke Wände unter Druckbeanspruchung (Load capacity of unreinforced concrete and masonry walls. Nonlinear calculation model and consistent design concept for slender walls under compressive stress)*. Dissertation, Technische Universität Darmstadt.

Haller, P. (1949) *Knickfestigkeit von Mauerwerk aus künstlichen Steinen (Buckling resistance of masonry made of artificial stone)*. Schweizerische Bauzeitung, 67(36), pp. 531-536

Holický, M. (2006) *Global resistance factors for concrete members*, Acta Polytechnica, CTU, Prague.

JCSS (2001) *Probabilistic Model Code*. Zurich: Joint Committee on Structural Safety, ISBN 978-3-909386-79-6.

Johnson, J. B., Bryan, C. W., Turneaure, F. E., Kinne, W. S. (1916) *The theory and practice of modern framed structures: Designed for the use of schools and for engineers in professional practice*. New York: John Wiley & Sons.

Kirtschig, K., Geldhaus, P., Gallenkemper, B., Schöner, W. (1975) *Aufbereitung eines Traglastverfahrens für den Mauerwerksbau. (Development of a load-bearing method for masonry construction)*

Kollbrunner, C. F., Meister, M. (1961) *Knicken, Biegedrillknicken, Kippen (Buckling, torsional buckling, tilting).* Theorie und Berechnung von Knickstaben Knickvorschriften. Berlin: Springer-Verlag.

Lehký, D., Keršner, Z. & Novák, D. (2014) *FraMePID-3PB Software for Material Parameters Identification Using Fracture Test and Inverse Analysis*. Advances in Engineering Software, Vol. 72, 147–54.

Moravík, M. Brodnan, M., Kotes, P., Kotula, P. (2012) *Skúsenosti s mostami zo starších typov prefabrikátov (Experience with older types of precast bridges)*. Betonárske dni 2012, zborník prednášok, STU v Bratislave, ISBN 978-80-8076-104-2, pp. 439-444.

Novák, D., Vořechovský, M., Teplý, B. (2014) *FReET: Software for the statistical and reliability analysis of engineering problems and FReET-D: Degradation module*. Advances in Engineering Software (Elsevier) 7: 179-192.

ÖNORM B 1992-1-1 (2011) *Bemessung und Konstruktion von Stahlbeton- und Spannbetontragwerken Teil 1-1: Grundlagen und Anwendungsregeln für den Hochbau.*

Pfeiffer, U. (2014) *Program: Analysis of Reinforced Concrete Structures*, TUHH, Version 2.90.

Quast, U. (2004) *Stützenbemessung*. In: Bergmeister, K. (Hg.): Beton-Kalender. Berlin: Ernst & Sohn.

Rosenblueth, E. (1981) *Two-point estimates in probabilities*. Appl. Math. Modelling, 5(329).

Řoutil, L., Lehký, D., Šimonová, H., Kucharczyková, B., Keršner, Z., Novák, T., Zimmermann, T., Strauss, A. & Krug B. (2014) *Experimental-computational determination of mechanical fracture parameters of concrete for probabilistic life-cycle assessment*. Proceedings of IALCCE 2014 – Fourth International Symposium on Life-Cycle Civil Engineering, Tokyo, Japan.

Strauss, A., Zimmermann, T., Lehký, D., Novák, D. & Keršner, Z. (2014) *Stochastic fracture-mechanical parameters for the performance-based design of concrete structures*. Struct. Concr. 15(3), 380–394.

Schlune, H., Plos, M., & Gylltoft, K. (2012) *Safety formats for non-linear analysis of concrete structures*. Magazine of Concrete Research, 64(7), 563-574.

Vořechovský, M. (2014) *Hierarchical refinement of Latin Hypercube Samples*. Computer-Aided Civil and Infrastructure Engineering, p. 1–18.

Zimmermann, T., Strauss, A., Lehký, D., Novák, D. & Keršner, Z. (2014) *Stochastic fracture-mechanical characteristics of concrete based on experiments and inverse analysis*. Constr build mater 73: 535–543

Zimmermann, T. and Lehký, D. (2015) *Fracture parameters of concrete C40/50 and C50/60 determined by experimental testing and numerical simulation via inverse analysis*. Journal of Fracture, 192(2):179–189.

Zimmermann, T., Lehký, D. and Strauss, A. (2016) *Correlation among selected fracture–mechanical parameters of concrete obtained from experiments and inverse analyses*. Structural Concrete, 17(6):1094–1103, 2016.